Heliyon 7 (2021) e08390

Contents lists available at ScienceDirect

Heliyon

journal homepage: www.cell.com/heliyon

Research article

A shorting-pin based compact meander multiband printed monopole antenna

Jeremiah O. Abolade [a,*], Dominic B.O. Konditi [b]

[a] Department of Electrical Engineering, Pan African University, Institute for Basic Sciences, Technology and Innovation, Nairobi, Kenya
[b] School of Electrical and Electronic Engineering, The Technical University of Kenya, Nairobi, Kenya

ARTICLE INFO

Keywords:
Shorting-pin based antenna
Compact meander antenna
Multiband printed monopole antenna

ABSTRACT

The antenna presented in this work is based on a meandering monopole patch antenna with the incorporated shorting-pin technique for the realization of multiband antenna. The proposed antenna is printed on an FR4 with a footprint of $0.22\lambda_g \times 0.36\lambda_g$ at the lowest operating frequency. The antenna proposed demonstrated six resonances with suitable bandwidth as well as gain which make it suitable for WiMAX, LTE-A, aeronautical radio navigation, sub6GHz band for 5G, and WLAN applications. The prototype of the proposed antenna is fabricated, measured, and presented. The comparative analysis of the proposed antenna with the recently reported works shows that the proposed antenna outperformed its counterpart in terms of size and number of bands. Therefore, the antenna reported in this work is a suitable and promising candidate for future portable mobile communication devices.

1. Introduction

Compact multiband antennas are in urgent need nowadays due to the heterogeneous nature of the wireless communication space and the portability of the users' equipment (UE). The cooperation of all the wireless technologies (2G, 3G, 4G, and 5G) and the varying countries' standards have contributed to the need for multiband antennas. Whereas various multi-band antennas have been reported in the literature, nonetheless, the compact multiband antenna is still a vast issue as demand for miniaturized devices keeps growing in the mobile market.

Many techniques have been explored in the literature for the miniaturization of multiband antennas. For example, slotting [1, 2, 3, 4, 5], Defected ground structure (DGS) [6, 7, 8, 9], parasitic loading [6, 10, 11, 12, 13, 14, 15], and multiple structure techniques have been used. Some of these structures have their disadvantages, for example, slotting (on the radiating patch) reduces the antenna gain and radiation efficiency; DGS can lead to complex structure; parasitic loading and multiple structure techniques increase the antenna size.

Furthermore, folded monopole antennas have drawn the attention of the antenna research community for miniaturizing antennas. For example, authors in [16] reported a tri-band monopole antenna using an open-end hexagonal radiating patch and ground plane stair slits. The antenna is suitable for a Global positioning system (GPS), Long term Evolution, and Satellite application on an FR4 substrate of $70 \times 45\text{mm}^2$. Authors in [17] proposed a tri-band tapered asymmetric coplanar fed monopole antenna with a complementary split-ring resonator (CSRR) at the ground plane side. The antenna was etched on a $25 \times 12.2\ \text{mm}^2$ FR4 having a permittivity of 4.4.

In recent times, the bio-inspired structure has also attracted antenna engineers due to its advantages such as perimeter improvement, fractality (self-repeating) nature, and flexibility. Whereas, majority of the bio-inspired antennas reported in the literature focus on ultrawideband applications [18, 19, 20, 21, 22], others have also explored it in developing compact multi-band antennas [4, 5, 23].

In this work, the concatenation of two meander lines and shorting pin techniques are used for the development of a compact Hexa-band antenna with the benefits such as low cost, scalable, compactness, and high number of operating bands when compared with recent works in the literature. The remaining sections are arranged as follows: the antenna design algorithm and analysis are presented in section 2, section 3 is the results and discussion, section 4 shows the parametric study of the proposed antenna, section 5 shows the comparative analysis, and the conclusion is presented in section 6.

2. Antenna design algorithm and analysis

The proposed antenna design is based on the concatenation of two meander lines and a shorting pin between the ground plane and radiating patch. Hereafter the proposed antenna is referred to as a printed monopole

* Corresponding author.
E-mail address: aboladejeremiah@yahoo.com (J.O. Abolade).

https://doi.org/10.1016/j.heliyon.2021.e08390
Received 9 October 2021; Received in revised form 29 October 2021; Accepted 10 November 2021

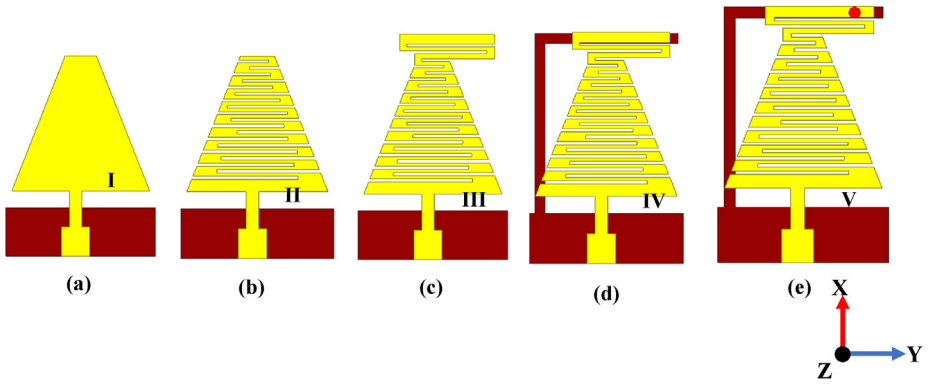

Figure 1. Step-by-step procedures for Designing the PMSP Antenna.

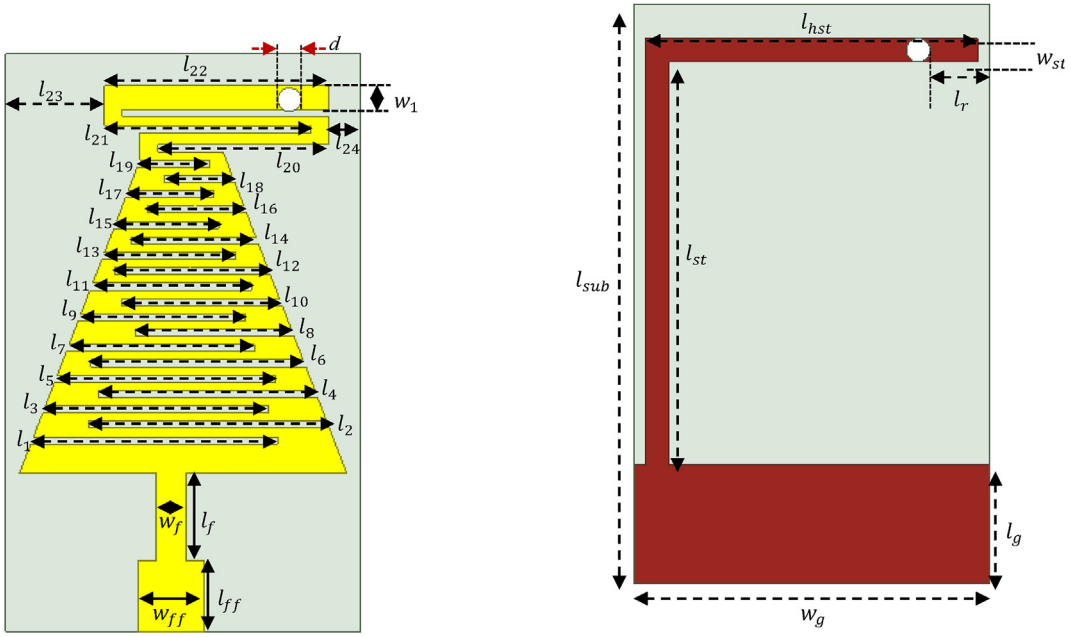

Figure 2. The PMSP antenna (a) top-view, and (b) bottom-view.

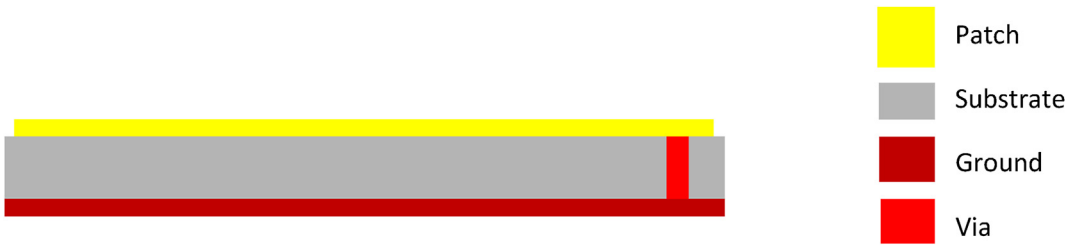

Figure 3. The front-view of PMSP antenna.

shorting-pin (PMSP) Antenna. The PMSP antenna is printed on an FR4 board with permittivity and thickness of 4.2 and 1.3mm respectively. The footprint of the PMSP antenna is 24 × 15mm^2 and it is fed with a 50Ω microstrip feedline. The design begins with a beveled Isosceles triangle as shown in Figure 1 (a). The beveled-isosceles triangle is converted to a beveled isosceles triangular shape meander-line through the use of varying rectangular shape slits as shown in Figure 1 (b). The S-shape meander line is then joined to the shape in Figure 1 (b) as shown in Figure 1 (c). An inverted L-shape stub was introduced to the ground plane. Finally, a 1mm diameter metal pin was used to join the radiating patch to the ground plane as shown in Figure 1 (e). Figure 2 (a), (b), and Figure 3 show the top-view, the bottom-view, and the front-view of the PMSP respectively. The optimized value of the design parameters is given in Table 1. A High-Frequency Structure Simulator (HFSS) which is built on the Finite Element Method (FEM) is used for the analysis of the PMSP antenna structure.

3. Results and discussion

3.1. Reflection coefficient

Ant. I demonstrated a -10dB resonance from 5.1GHz as can be seen in Figure 4 but with the introduction of slits (ANT. II), the first resonance

Table 1. Optimized design parameters of PMSP antenna.

Parameter	l_1	l_2	l_3	l_4	l_5	l_6	l_7	l_8	l_9	l_{10}
Value (mm)	10.4	10.2	9.5	9.1	9.2	9.0	7.8	6.6	6.9	6.7
Parameter	l_{11}	l_{12}	l_{13}	l_{14}	l_{15}	l_{16}	l_{17}	l_{18}	l_{19}	l_{20}
Value (mm)	6.7	6.5	5.5	5.3	4.3	4.1	3.6	2.9	2.9	7.25
Parameter	l_{21}	l_{22}	l_{23}	l_{24}	l_f	l_{ff}	l_{sub}	l_{st}	l_{hst}	l_r
Value (mm)	8.75	9.5	4.2	1.3	3.7	3	24	17	11.5	2.5
Parameter	l_g	w_f	w_{ff}	w_1	w_{st}	w_g	d			
Value (mm)	5	1.25	2.8	1	1	15	1			

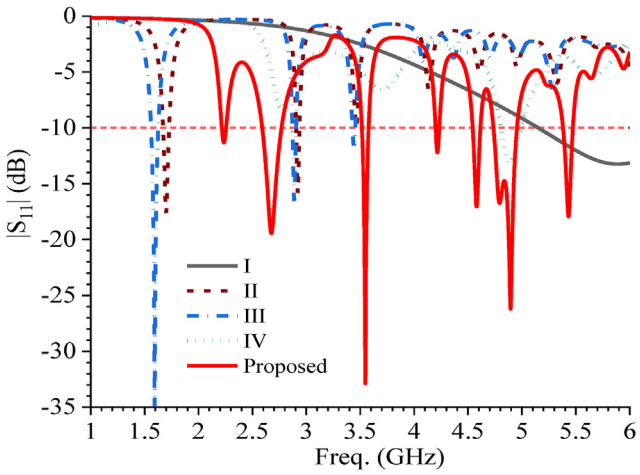

Figure 4. $|S_{11}|$ of the PMSP antenna.

below -10dB occurred at 1.7GHz and another resonance at 2.9GHz with a reflection coefficient of -18dB and -17dB respectively which is suitable for LTE and S-band applications. This shows a 70.7% reduction compared with Ant. I. The concatenation of the S-shaped meander line (ANT. III) results in the shift of resonance frequency with a better return loss as seen in Figure 4. Ant. IV shows a poor impedance matching across the bands except at 5.1GHz as shown in Figure 4. Finally, the use of via (PMSP antenna) results in hepta-bands antenna resonating at 2.2GHz, 2.6GHz, 3.5GHz, 4.2GHz, 4.6GHz, 4.9GHz, and 5.4GHz with a $|S_{11}|$ of -12dB, -20dB,-34dB, -13dB, -18dB, -27dB, and -18dB respectively. The prototype of the PMSP antenna is fabricated and measured as seen in Figure 5. It can be seen from Figure 6 that apart from the second band, there is no significant difference between the measured and simulated $|S_{11}|$ results. It can be seen from the measured result that for $|S_{11}| \leq$-10dB, the prototype antenna resonates at 2.2GHz, 3.5GHz, 4.2GHz, 4.6GHz, 4.95GHz, and 5.6GHz which means that the PMSP antenna can be said to be a Hexa-band antenna which is suitable for WiMAX, LTE-A, aeronautical radio navigation, sub6GHz band for 5G, and WLAN applications.

3.2. Gain, radiation pattern, and surface current distribution of the PMSP antenna

Figure 7 shows the gain of the PMSP antenna. It can be observed that the PMSP antenna has suitable gain in all the operating frequencies with

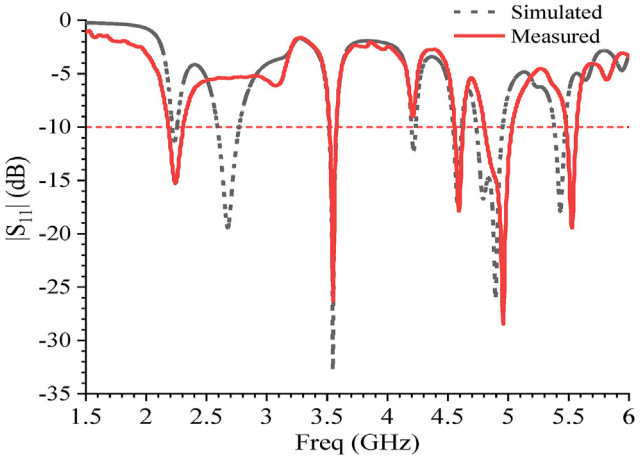

Figure 6. Measured and simulated |S11| of the PMSP Antenna.

Figure 5. The prototype of the PMSP Antenna.

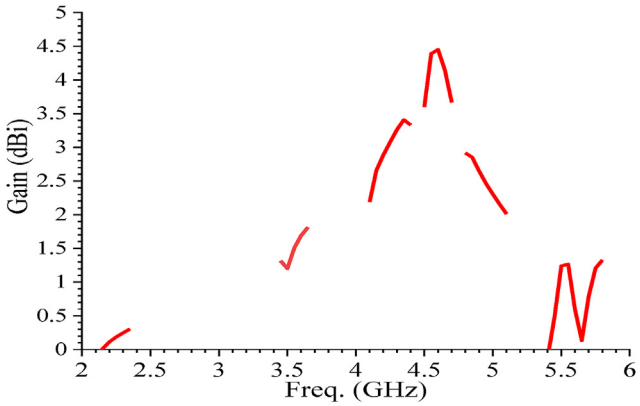

Figure 7. Gain of the PMSP antenna.

the lowest at the lowest frequency band and the highest in the fourth band with a peak gain of 4.6 dBi. This shows that the PMSP antenna is applicable in the aforesaid applications owing to its gain response in all the operating frequencies.

The radiation pattern of the PMSP antenna is shown in Figure 8. It can be observed that the E-Plane radiation patterns at (denoted by the red short-dash) 2.2GHz, and 4.6GHz are bidirectional, omnidirectional at 3.5GHz, and quasi-omnidirectional at 4.2GHz, 4.9GHz, and 5.6GHz respectively. The H-plane (denoted by the blue solid line) radiation pattern of the PMSP antenna is omnidirectional at all the operating frequencies except at 4.6GHz which has a quasi-omnidirectional radiation pattern a shown in Figure 8.

The operation of an antenna can better be understood through the antenna current distribution. It helps in showing which part of the antenna is responsible for certain resonance and it clearly shows the antenna electrical length (l_e) as shown in Eq. (1). Hence, the current distribution of the PMSP antenna at 2.2GHz, 3.5GHz, 4.2GHz, 4.6GHz, 4.95GHz, and 5.6GHz are as shown in Figure 9.

$$f_r = \frac{c}{2L_e\sqrt{\varepsilon_{eff}}} \tag{1}$$

Where; f_r is the resonance frequency, c is the free space velocity, L_e is the electrical length and ε_{eff} is the effective permittivity of the substrate.

It can be observed that the stub of the ground plane has different contributions at a different frequency as seen in Figure 9. It can also be observed in FIG that different slit has different responses at different frequencies.

4. Parametric study of PMSP

The effect of the ground length (l_g), shorting-pin location (l_r), and the length of the horizontal stub (l_{hst}) on the resonance response of PMSP are studied and presented in this section.

4.1. The effect of the length of the ground (l_g) on $|S_{11}|$

Figure 10 shows the effect of l_g on the resonance response of the proposed antenna. As can be seen in Figure 10, l_g has greater effect on $|S_{11}|$. For instance, when $l_g = 6mm$, the antenna only maintains a Quad-band with $|S11| < -10dB$ compared to when it is $5mm$ which is an hepta-band with $|S11| < -10dB$. It can be observed that the PMSP becomes a dual band with $l_g = 7mm$. It can be deducted from Figure 10 that the optimized result is achieved when $l_g = 5mm$.

4.2. The effect of the shorting-pin location (l_r) on $|S_{11}|$

It can be observed from Figure 11 that l_r has tunning effect on all the resonance frequencies except the second resonance. It can be observed that as l_r increases the lowest resonance frequency increases which shows that there is a reduction in the effective length of the PMSP antenna. It can also be seen in Figure 11 that the 2.2GHz band resonance is lost when $l_r = 10.5mm$. This shows that the location of the shorting-pin is very critical in PMSP antenna. It can be observed that the optimized value of l_r is 2.5mm because it demonstrated good impedance matching across the entire resonances.

4.3. The effect of the length of the horizontal stub (l_{hst}) on $|S_{11}|$

Figure 12 shows the $|S_{11}|$ variation with respect to l_{hst}. It can be observed that as l_{hst} increases, the resonance frequencies decreases but at the expense of reduction in the return loss at the fundamental frequency.

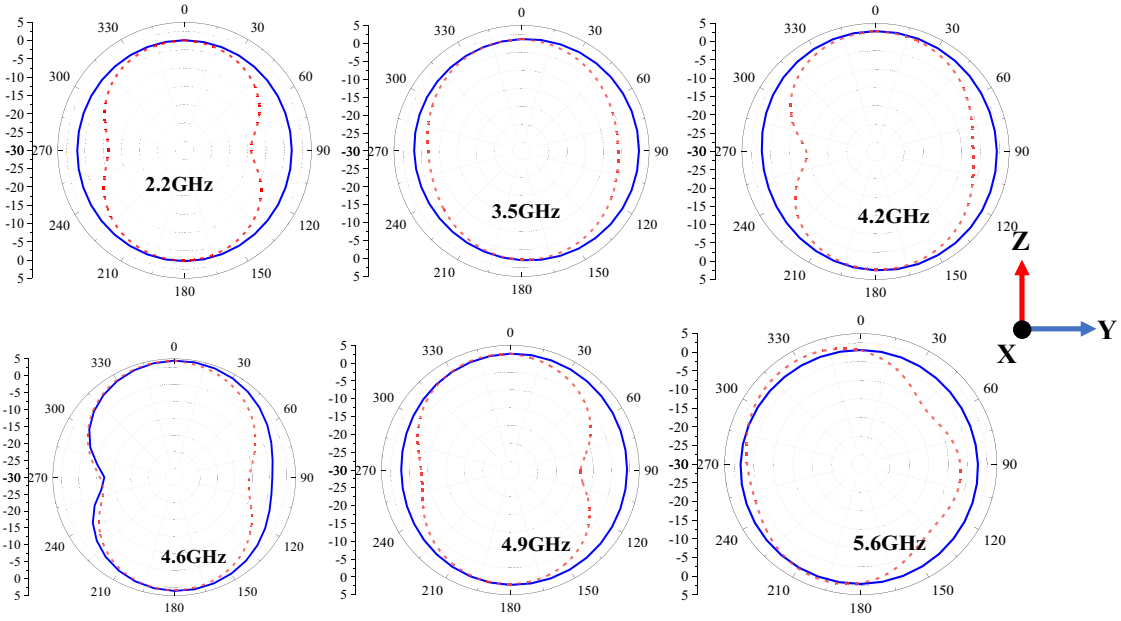

Figure 8. Radiation pattern of the PMSP Antenna.

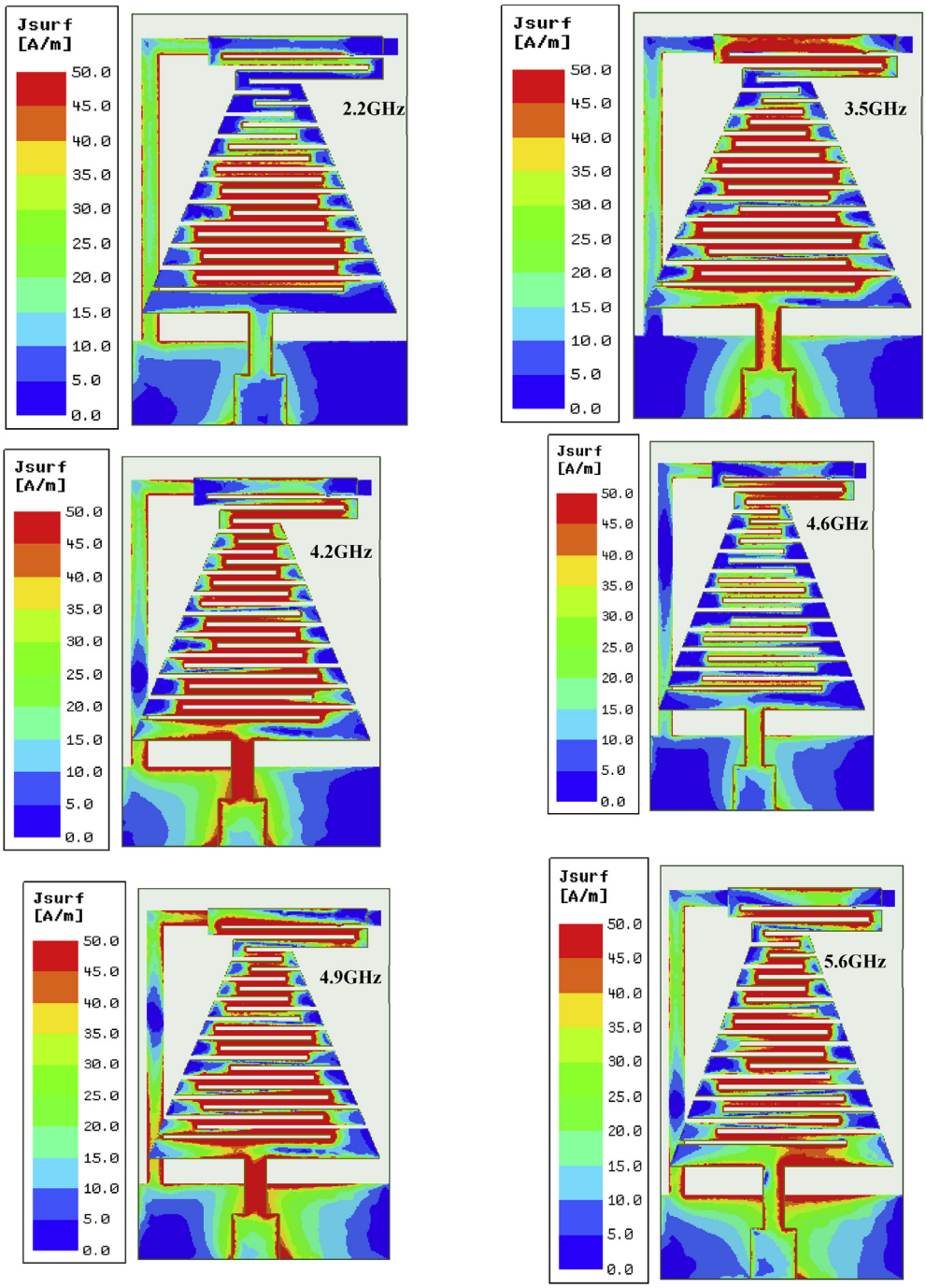

Figure 9. Current distribution of the PMSP Antenna.

The shift in frequency is more pronounced at the fundamental frequency, third, fifth and sixth resonances as can be seen in Figure 12. It can be observed that although the return loss at the fundament frequency is low when l_{hst} is 11.5mm yet the return loss at the fifth, sixth, and seventh resonance which shows that 11.5mm is the optimal value of l_{hst} for the proposed PMSP antenna.

5. Comparative analysis of PMSP antenna

In this section, the proposed antenna is compared with the existing works in the literature and presented in Table 2. Guided wavelength sizing is used for normalization purposes. The sizes are done using the lowest resonance frequency. It can be observed that though the antenna reported in [24] is comparatively small nonetheless it is a dual-band antenna while the antenna proposed in this work is a Hexa-band antenna. It can also be seen that even though the PMSP antenna is comparatively smaller yet it has the highest number of operating bands as well as suitable gain.

6. Conclusion

In this work, a compact Hexa-band antenna based on the concatenation of two meander lines and a shorting pin between the ground plane and radiating patch. The footprint of the PMSP antenna is $24 \times 15\text{mm}^2$. The prototype of the PMSP antenna is fabricated, measured, and reported. The PMSP antenna is a Hexa-band antenna that is suitable for

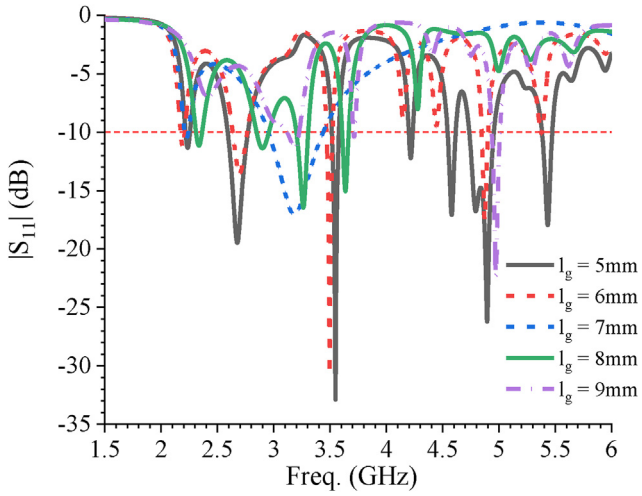

Figure 10. $|S_{11}|$ response with respect to l_g of the PMSP Antenna.

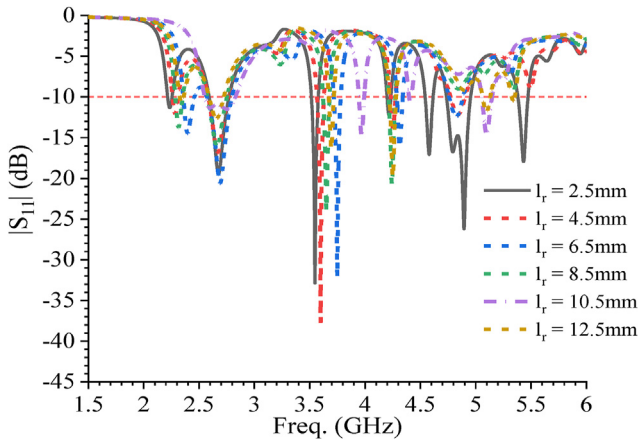

Figure 11. $|S_{11}|$ response with respect to l_r of the PMSP Antenna.

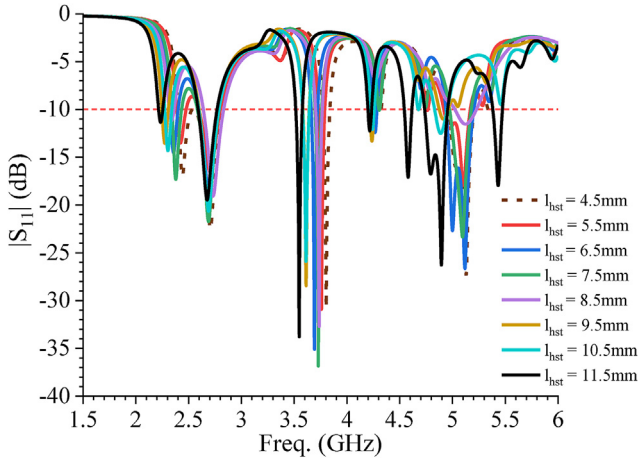

Figure 12. $|S_{11}|$ response with respect to l_{hst} of the PMSP Antenna.

WiMAX, LTE-A, aeronautical radio navigation, sub6GHz band for 5G, and WLAN applications. The comparative analysis shows that the PMSP antenna has benefits such as low cost, scalable, compactness, and a high number of operating bands compared with recent works in the literature.

Table 2. Comparative analysis of the PMSP antenna.

Ref	Year	Size (λ_g^2)	Freq. (GHz)	BW(MHz)	Gain	Methodology
[25]	2018	0.38 × 0.42	2.48/ 3.49	340/390	2.4/3.5 (dB)	Meandering, SSR, and CPW
[24]	2019	0.26 × 0.17	1.22/ 6.06	40/2360	0.99/ 3.72 dBi	CRLH-TL, CPW
[26]	2019	0.50 × 0.52	2.4/3.5	200/390	2.25/ 0.88 (dBi)	MTM
[27]**	2020	0.42 × 0.49	3.59/ 5.53^{+}	2830	3/3.6 dBi	C-SRR, H-CRR and ACGP
[28]	2020	0.42 × 0.77	0.85/ 1.8/2.6	NR	10 dB$^{\#}$	Folded monopole with SRR
[29]	2020	0.73 × 0.25	0.9/ 1.95/ 5.8	NR	3.2/3.8/ 9.2 dBi	Folded branch with slit
This work		0.22 × 0.36	2.2/3.5/ 4.2/4.6/ 4.9/5.6	120/60/ 30/60/ 230/80	0.4/1.7/ 3.4/4.6/ 2.8/1.1 dBi*	Hybrid Meander lines and shorting-pin

*Peak value, $^{+}$Range, $^{\#}$Diversity gain, $^{+}$Extracted from the comparative table, SSR- Square Split Ring; CPW- Co-planar waveguide; MTM- Metamaterial; C-SRR- Complementary Split Ring Resonator; H-CRR- Hexagonal Closed Ring Resonator; ACGP- Asymmetric coplanar ground plane; NR- Not reported; **wideband antenna with two resonances.

Declarations

Author contribution statement

Jeremiah O. Abolade: Conceived and designed the experiments; Performed the experiments; Analyzed and interpreted the data; Wrote the paper.

Dominic B. O. Konditi: Analyzed and interpreted the data; Wrote the paper.

Funding statement

This work was supported by the African Union through the Pan African University Institute of Basic Sciences, Technology, and Innovation.

Data availability statement

No data was used for the research described in the article.

Declaration of interests statement

The authors declare no conflict of interest.

Additional information

No additional information is available for this paper.

References

[1] K.D. Prasad, T. Ali, R.C. Biradar, A compact slotted multiband antenna for L-band and WLAN applications, in: 2017 2nd IEEE International Conference on Recent Trends in Electronics, Information & Communication Technology (RTEICT), 2017, pp. 820–823.

[2] R. Parikh, B. Singh, Effects of slots on resonant frequencies of a microstrip patch antenna, in: 2018 Fourth International Conference on Computing Communication Control and Automation, ICCUBEA, 2018, pp. 1–5.

[3] D. Chang, J. Liu, B. Zeng, C. Wu, C. Liu, A.D. Operations, Compact Double-Ring Slot Antenna with Ring-Fed for Multiband Applications, no. 2, 2006, pp. 2–6.
[4] J.O. Abolade, D.B.O. Konditi, V.M. Dharmadhikary, Compact hexa-band bio-inspired antenna using asymmetric microstrip feeding technique for wireless applications, Heliyon 7 (2) (2021) e06247.
[5] J.O. Abolade, D.B.O. Konditi, V.M. Dharmadhikary, A comparative study of compact multiband bio-inspired asymmetric microstrip fed antennas (BioAs-MPAs) for wireless applications, J. Eng. 2021 (2021) 1–17.
[6] T.K. Das, B. Dwivedy, S.K. Behera, Design of a meandered line microstrip antenna with a slotted ground plane for RFID applications, AEU - Int. J. Electron. Commun. 118 (2020) 153130.
[7] R. Hussain, M.U. Khan, M.S. Sharawi, An integrated dual MIMO antenna system with dual-function GND-plane frequency-agile antenna, IEEE Antenn. Wireless Propag. Lett. 17 (1) (2018) 142–145.
[8] A. Yadav, S. Goyal, T. Agrawal, R.P. Yadav, Multiband antenna for Bluetooth/ZigBee/Wi-Fi/WiMAX/WLAN/X-band applications: partial ground with periodic structures and EBG, in: 2016 International Conference on Recent Advances and Innovations in Engineering, ICRAIE, 2016, pp. 1–5.
[9] R. Mark, N. Mishra, K. Mandal, P.P. Sarkar, S. Das, Hexagonal ring fractal antenna with dumb bell shaped defected ground structure for multiband wireless applications, AEU - Int. J. Electron. Commun. 94 (2018) 42–50.
[10] W. Chen, Y. Yao, J. Yu, X. Liu, X. Chen, Design of a novel multiband antenna for mobile terminals, in: 2015 IEEE International Wireless Symposium, IWS 2015, 2015, pp. 1–4.
[11] M. Rezvani, Y. Zehforoosh, A dual-band multiple-input multiple-output microstrip antenna with metamaterial structure for LTE and WLAN applications, AEU - Int. J. Electron. Commun. 93 (2018) 277–282.
[12] H. Liu, B. Lu, L. Li, Novel miniaturized octaband Antenna for LTE smart handset applications, Int. J. Antenn. Propag. 2015 (2015) 1–9.
[13] Y. Yan, Y. Jiao, W. Zhang, Design of an X-band Antenna on airborne craft with omnidirection radiation, in: 2018 12th International Symposium on Antennas, Propagation and EM Theory, ISAPE, 2018, pp. 1–2.
[14] C. Sim, C. Yeh, H. Lin, Compact size triple-band monopole antenna with parasitic element for WLAN/WiMAX applications, in: 2014 International Symposium on Antennas and Propagation Conference Proceedings, 2014, pp. 469–470.
[15] Y. Li, Q. Chu, Compact eight-band monopole for LTE mobile phone, in: 2020 14th European Conference on Antennas and Propagation, EuCAP, 2020, pp. 1–3.
[16] M.A. Al-Mihrab, A.J. Salim, J.K. Ali, A compact multiband printed monopole antenna with hybrid polarization radiation for GPS, LTE, and satellite applications, IEEE Access 8 (2020) 110371–110380.
[17] V. Rajeshkumar, R. Rengasamy, P.V. Naidu, A. Kumar, A compact meta-atom loaded asymmetric coplanar strip-fed monopole antenna for multiband operation, AEU - Int. J. Electron. Commun. 98 (2019) 241–247.
[18] P.F. Da Silva, R.C.S. Freire, A.J.R. Serres, P.H. da F. Silva, J.C. e Silva, Bio-inspired antenna for UWB systems, in: 1st International Symposium on Instrumentation Systems, Circuits and Transducers, INSCIT, 2016, pp. 1–5.
[19] A.K. Ebnabbasi, bio-inspired printed-antenna transmission-range detection systems, IEEE Antenn. Propag. Mag. 55 (2013) 193–200.
[20] J.O. Abolade, D.B.O. Konditi, V.M. Dharmadhikary, Bio-inspired wideband antenna for wireless applications based on perturbation technique, Heliyon 6 (June) (2020) e04282.
[21] P.F. Da-Silva-Júnior, et al., Bio-inspired wearable antennas, in: Wearable Technologies, Intech, Janeza Trdine 9, 51000 Rijeka, Croatia, 2018, pp. 219–237.
[22] J.O. Abolade, D.B.O. Konditi, V.M. Dharmadhikary, Compact vitis vinifera- inspired ultrawideband Antenna for high-speed communications, Int. J. Antenn. Propag. 2021 (2021).
[23] J.O. Abolade, D.B.O. Konditi, V.M. Dharmadhikary, Ultra-compact hexa-band bio-inspired antenna for 2G , 3G , 4G and 5G wireless applications, Int. J. Commun. Antenna Propag. 11 (3) (2021) 1–13.
[24] R. Sonak, M. Ameen, R.K. Chaudhary, CPW-fed electrically small open-ended zeroth order resonating metamaterial antenna with dual-band features for GPS/WiMAX/WLAN applications, AEU - Int. J. Electron. Commun. 104 (2019) 99–107.
[25] K. Kumar Naik, Asymmetric CPW-fed SRR patch antenna for WLAN/WiMAX applications, AEU - Int. J. Electron. Commun. 93 (2018) 103–108.
[26] M.M. Hasan, M. Rahman, M.R.I. Faruque, M.T. Islam, M.U. Khandaker, Electrically compact srr-loaded metamaterial inspired quad band antenna for bluetooth/wifi/wlan/wimax system, Electron 8 (2019) 7.
[27] M. Ameen, A. Mishra, R.K. Chaudhary, Asymmetric CPW-fed electrically small metamaterial- inspired wideband antenna for 3.3/3.5/5.5 GHz WiMAX and 5.2/5.8 GHz WLAN applications, AEU - Int. J. Electron. Commun. 119 (2020) 153177.
[28] S.S. Alja'Afreh, Q. Xu, L. Xing, Y. Huang, C. Song, E. Almajali, A dual-element folded strip monopole with SRR loading for multiband handset MIMO applications, in: 2020 14th European Conference on Antennas and Propagation, EuCAP, 2020, pp. 1–5.
[29] J. Cui, A. Zhang, X. Chen, An omnidirectional multiband Antenna for railway application, IEEE Antenn. Wireless Propag. Lett. 19 (1) (2020) 54–58.